ARTICLES
https://doi.org/10.1038/s41594-020-00515-z

nature structural & molecular biology

The three-dimensional structure of human β-endorphin amyloid fibrils

Carolin Seuring[1,2,7], Joeri Verasdonck[1,7], Julia Gath[1], Dhimam Ghosh[1,3], Nadezhda Nespovitaya[1], Marielle Aulikki Wälti[1], Samir K. Maji[3], Riccardo Cadalbert[1], Peter Güntert[1,4,5], Beat H. Meier[1]✉ and Roland Riek[1,6]✉

In the pituitary gland, hormones are stored in a functional amyloid state within acidic secretory granules before they are released into the blood. To gain a detailed understanding of the structure–function relationship of amyloids in hormone secretion, the three-dimensional (3D) structure of the amyloid fibril of the human hormone β-endorphin was determined by solid-state NMR. We find that β-endorphin fibrils are in a β-solenoid conformation with a protonated glutamate residue in their fibrillar core. During exocytosis of the hormone amyloid the pH increases from acidic in the secretory granule to neutral level in the blood, thus it is suggested—and supported with mutagenesis data—that the pH change in the cellular milieu acts through the deprotonation of glutamate 8 to release the hormone from the amyloid. For amyloid disassembly in the blood, it is proposed that the pH change acts together with a buffer composition change and hormone dilution. In the pituitary gland, peptide hormones can be stored as amyloid fibrils within acidic secretory granules before release into the blood stream. Here, we use solid-state NMR to determine the 3D structure of the amyloid fiber formed by the human hormone β-endorphin. We find that β-endorphin fibrils are in a β-solenoid conformation that is generally reminiscent of other functional amyloids. In the β-endorphin amyloid, every layer of the β-solenoid is composed of a single peptide and protonated Glu8 is located in the fibrillar core. The secretory granule has an acidic pH but, on exocytosis, the β-endorphin fibril would encounter neutral pH conditions (pH 7.4) in the blood; this pH change would result in deprotonation of Glu8 to release the hormone peptide from the amyloid. Analyses of β-endorphin variants carrying mutations in Glu8 support the role of the protonation state of this residue in fibril disassembly, among other environmental changes.

Functional amyloids exist in fungi, bacteria, insects and humans[1–5]. They are involved in adhesion, invasion and biofilm formation, exhibit regulatory functions and act in the sorting and storage of hormone peptides. β-endorphin amyloids belong to the last group of functional amyloids. β-endorphin is an endogenous opioid neuropeptide of the central nervous system and the pituitary gland. It is involved in the regulation of the stress response and pain perception, and is activated during exercise[6]. As with many other pituitary hormones, β-endorphin is secreted by the so-called 'regulated' secretory pathway[7,8], through which cells are able to store peptide or protein entities for extended periods of time by concentrating the secretory peptides or proteins inside membrane-enclosed secretory granules[7,9,10]. When a signal triggers their release, peptides or proteins are secreted into the blood much faster than their synthesis rates would permit, yielding a fast and intense signaling event. The granules are generally composed of a single peptide or protein species stored in an amyloid state[11], which has been structurally characterized for several peptide hormones[12,13].

The amyloid structure confers semi-autonomous properties for peptide and protein sorting, secretory granule formation, inert storage and peptide or protein release, minimizing the need for a dedicated cell machinery[5]. However, the chemical environment (including pH, phosphate and cofactors) appears to play an important role in hormone assembly inside secretory granules and during their disassembly into the blood stream[11]. Indeed, the decrease of phosphate salt from about 60 mM in the cytosol to about 1–2 mM phosphate in the blood has been suggested to support disassembly of β-endorphin amyloid fibrils[14]. Furthermore, a concomitant decrease in the concentration of heparin, which is several orders of magnitude higher in secretory granules than in the blood, may promote the disintegration of β-endorphin amyloid fibrils[14,15].

To get detailed mechanistic insights into the disassembly of the amyloid entity, we determined here the atomic-resolution structure of the β-endorphin amyloid fibril by solid-state NMR and performed mutagenesis and fibril disassembly studies. The resulting structure–function relationship of peptide release from amyloid fibrils shows the nature of the interplay between cellular environment and amyloid structure and stability, building a basis for understanding the mechanism of secretory granule formation and hormone release in vivo.

Results

Fibril formation by β-endorphin under physiological conditions. The β-endorphin fibrils in this study were grown under physiological conditions, namely at pH 5.5 and in the presence of 400 µM low molecular weight (LMW) heparin. The pH of 5.5 was selected to mimic the pH of secretory granules[16] and heparin was used as a representative for glycosaminoglycans, which are present at high

[1]Laboratory of Physical Chemistry, ETH Zürich, Zürich, Switzerland. [2]Center for Free-Electron Laser Science, Deutsches Elektronen-Synchrotron, Hamburg, Germany. [3]Department of Biosciences and Bioengineering, IIT Bombay, Powai, Mumbai, India. [4]Institute of Biophysical Chemistry, Center for Biomolecular Magnetic Resonance, Goethe University Frankfurt am Main, Frankfurt am Main, Germany. [5]Graduate School of Science, Tokyo Metropolitan University, Tokyo, Japan. [6]Structural Biology Laboratory, The Salk Institute, La Jolla, CA, USA. [7]These authors contributed equally: Carolin Seuring, Joeri Verasdonck. ✉e-mail: beme@ethz.ch; roland.riek@phys.chem.ethz.ch

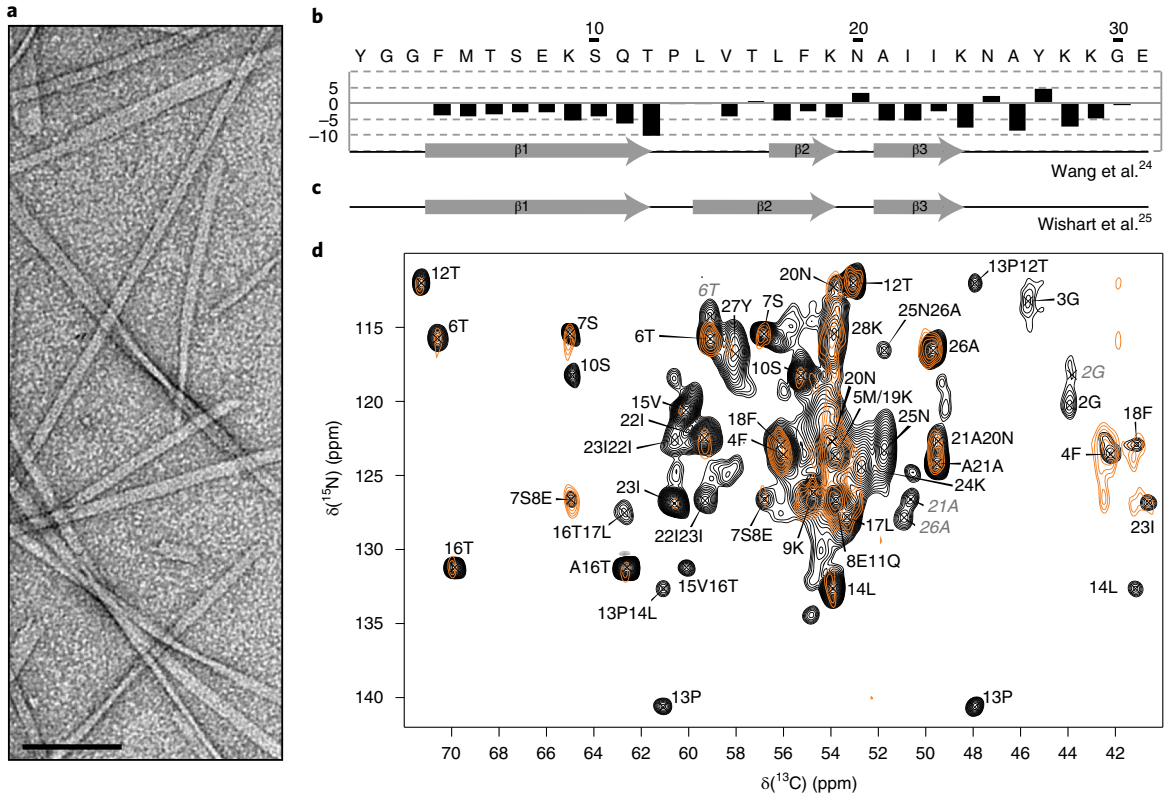

Fig. 1 | Initial structural characterization of β-endorphin amyloid fibrils. a, Negative-stain transmission electron micrograph of micrometer-long, unbranched β-endorphin fibrils. The scale bar is 200 nm. **b**, Predicted secondary structure of the β-endorphin peptide in its amyloid state based on backbone ($\Delta\delta^{13}C^{\alpha}$-$\Delta\delta^{13}C^{\beta}$) (ppm) secondary chemical shifts[24]. For Gly, $\Delta\delta^{13}C^{\alpha}$ values are plotted. Three β-strands are labeled with β1, β2 and β3. **c**, An alternative secondary-structure prediction based on other random-coil chemical-shift values[25]. **d**, Superposition of the NCA spectrum (^{15}N to ^{13}CA correlation spectrum) of uniformly ^{15}N, ^{13}C-labeled fibrils (black) with the PAIN spectrum of mixed fibrils composed of exclusively ^{15}N or ^{13}C-labeled monomers (orange). The superposition of cross peaks indicates in-register parallel β-sheets. Individual cross peaks are assigned with sequence positions and amino acid single letter codes.

abundance in secretory granules[17] and may affect neuropeptide aggregation. Under these conditions, we previously obtained a single set of very well-defined solid-state NMR resonances[18], indicating the presence of a single polymorph.

This polymorph was stable (as assessed by solid-state NMR) under different buffer conditions; that is, with 10 mM NH_4Ac and 200 mM NaCl or with 5% D-mannitol in addition to heparin[19]. A single polymorph that is stable under different conditions has been observed with other functional amyloid systems, such as the HET-s(218–289) prion[20,21]. However, there was an apparent chemical-shift difference between the solid-state NMR spectra of heparin-containing and heparin-free fibrils, suggesting considerable structural differences between the two preparations[14]. In addition, β-endorphin fibrils grown in the absence of heparin show multiple polymorphs, suggesting that heparin influences the coherence length of the fiber[14]. This is in agreement with super-resolution fluorescence microscopy studies that showed that heparin acts as a structural component of β-endorphin amyloid fibrils, rather than a simple aggregation promoter[14,15].

β-endorphin monomers pack into in-register parallel β-sheets. In the presence of heparin β-endorphin forms micrometer-long unbranched fibrils (Fig. 1a)[19], which were sedimented into 3.2-mm NMR rotors. The fibrils are composed of several protofibrils (Fig. 1a) with a mass per length (MPL) of 16.6 kDa nm^{-1}, corresponding to one molecule per cross-β sheet layer of the protofibril[19] and exhibit a cross-β diffraction[22]. The NMR sequential resonance assignment was previously obtained using a set of 3D experiments[18] and reported[23] (Biological Magnetic Resonance Bank (BMRB) entry 26715). All residues except Tyr1 and Gly2 were visible in the spectrum. The line width of most ^{13}C peaks was ~120 Hz, consistent with a well-ordered system.

The secondary structure was derived from chemical shifts, which indicate the presence of three β-strands, formed by residues 4–12 (β1), (14)17–19 (β2) and 21–24 (β3) (Fig. 1b). The length of β2 varies according to the reference chemical-shift set used[24,25] (Fig. 1b,c), and in the following, we use the more conservative classification, β2:17–19.

Most amyloids of biologically relevant systems characterized so far are organized into in-register parallel β-sheets[26]. To verify this hypothesis for β-endorphin amyloids, a proton assisted insensitive nuclei cross polarization (PAIN) experiment on a 1:1 mixture of exclusively ^{13}C and ^{15}N-labeled peptides was performed[27]. For an in-register parallel arrangement, PAIN peaks are expected at the same positions as ^{15}N-^{13}CA correlations retrieved from a uniformly labeled sample. Indeed, strong peaks for N-C contacts in the 1:1 mixture were found for a number of residues covering all three β-sheets (Supplementary Table 1), strongly indicating the presence of an in-register parallel β-sheet structure.

Collection of distance restraints for 3D structure calculation. We used a 500-μs mixing time CHHC(^{13}C-^{1}H to ^{1}H-^{13}C correlation)[28], a 6.5-ms PAR (proton-assisted recoupling)[29] and a 400-ms PDSD (proton-driven spin diffusion)[30,31] experiment (Extended Data Fig. 1 and Supplementary Figs. 1 and 2) on a uniformly ^{15}N,^{13}C-labeled fibril sample to identify through-space contacts from the cross-peak

positions using the program CcpNmr Analysis[32]. We selected cross peaks with a single assignment based on the chemical shifts (spectrally unambiguous peaks) as well as peaks with low assignment ambiguity (Supplementary Table 2).

To distinguish between intra- and intermolecular restraints among the low ambiguity peaks we compared the three aforementioned spectra with identical spectra acquired on samples with 20% labeled monomers mixed with 80% monomers with natural isotopic abundance[27] (Extended Data Fig. 2 and Supplementary Table 2). The experimental parameters are given in Supplementary Table 3. In contrast to other fibrils investigated[27,33,34], only few of the peaks could be classified unambiguously following the procedure described in the caption of Extended Data Fig. 2, hinting at a staggered arrangement of the molecules. This is in agreement with the mean weighted cross-peak intensities for residue pairs of 0.5 on average, which are between the values of 1 and 0.2 representative for an entirely intramolecular or entirely intermolecular cross-peak, respectively.

In earlier studies (in particular with fibrils of MPL of >1)[27,33,34], it was necessary to first calculate a structure on the basis of these low ambiguity restraints and their further classification of the restraints as intra- or intermolecular. However, in the present case, with an MPL of 1 and well-resolved solid-state NMR spectra, this initial calculation has proved unnecessary (although it was still performed).

3D structure calculation. With this set of 192 distance restraints (Table 1 and Supplementary Table 2), a 3D structure of the β-endorphin protofibril with one molecule per layer[19] was calculated using CYANA[35,36]. For structure calculations, the amyloid protofibril was approximated by six β-endorphin molecules. Symmetry restraints[37] were applied to enforce identical structures for the six monomers.

Intermolecular hydrogen-bond restraints corresponding to in-register β-sheets were introduced for the β-strands of residues 4–12 (β1), 17–19 (β2) and 21–24 (β3) (Fig. 1b). Backbone dihedral angles were restrained to $-200° < \varphi < -80°$ and $40° < \psi < 220°$ if the difference of the C^{α} and C^{β} secondary chemical shifts was below −2 ppm for three residues in a row[38]. Intermolecular hydrogen-bond restraints were added to ensure the in-register parallel packing of adjacent β-strands into a β-sheet. Four possibilities for the relative orientation of the three β-strands exist. Calculating 3D structures with all the experimental distance restraints for all four possible packings showed that only one orientation yielded low CYANA target function values (Extended Data Fig. 3b) and thus only one orientation is compatible with the experimental data set. It is the one for which the hydrogen bonds of β-sheet β2 have opposite orientations along the fibril axis with respect to the β-sheets β1 and β3 (noted ABA or BAB in the Extended Data Fig. 3b), which was then used in the following calculations.

The structure calculation used the manually identified restraints of Supplementary Table 2 and a further 1,830 cross peaks selected in the CHHC, PAR and PDSD spectra of the β-endorphin samples in the presence of 10 mM NH_4Ac, 200 mM NaCl, 400 µM LMW heparin (buffer A). Of these, 1,261 were iteratively assigned to interatomic distances by CYANA[35] using the known resonance assignment[23]. The calculated structure is shown in Fig. 2a. The bundle composed of ten conformers (Fig. 2b) fulfills the conformational restraints with an average CYANA target function of 2.97 Å^2 and is well-defined with an average r.m.s.d. to the mean coordinates of residues 3–27 of the hexamer of 0.39 Å for the backbone atoms N, C^{α}, C′ and 0.71 Å for the heavy atoms (Table 1).

The 3D structure of β-endorphin protofibrils is a β-solenoid. The 3D structure of the β-endorphin fibril shows a β-solenoid composed of three in-register parallel β-sheets around the central fiber axis (Fig. 3a) with the longest dimension of the protofibril (~3.3 nm) similar to the protofibril width previously determined by electron microscopy[14] (~3.2 nm) (Extended Data Fig. 4). Every layer of the solenoid is made by one peptide (individually colored in Fig. 3) unlike the β-solenoid of the HET-s(218–289) prion[27,39], which has two layers per protein. In the 3D structure, β-strands are formed by residues 4–10 (β1), 14–19 (β2) and 21–24 (β3) as determined by hydrogen bonding supporting backbone geometries. Their lengths differ slightly from those suggested by chemical-shift-based secondary-structure prediction (Fig. 1b). The β1 and β2 strands interact through a hydrophilic core comprising the side chains of Thr6, Glu8, Ser10 and Thr16 and with the hydrophobic side chains of Phe4 and Phe18, the latter being part of the central hydrophobic core that includes also Ala21, Ile23 and Ala26 of strand β3 (Fig. 3c,d). Side chains of opposing β-strands β1 and β2 are staggered at the turn between Ser10 and Pro13 (Fig. 3e–g), while the staggering of the aromatic residues Phe4 and Phe18 is of intramolecular nature (Fig. 3h; also supported by the lack of intermolecular cross peaks between Phe4 and Phe18). Ser10, Thr12 and Thr16 form hydrogen-bonded ladders as typically observed in amyloids[40].

Table 1 | NMR and structure statistics

	β-endorphin protofibril (BMRB 26715, PDB 6TUB)
NMR distance and dihedral constraints (per monomer)	
Distance restraints from solid-state NMR	
Manually assigned in CHHC/PAR/PDSD ($\|i-j\|>2$)	49 / 73 / 70
Spectrally unambiguous	16 / 28 / 30
Manually assigned intramolecular	6 / 11 / 2
Manually assigned intermolecular	8 / 3 / 19
Total manually and automatically assigned	714
Intraresidue ($\|i-j\|=1$)	118
Interresidue	
Medium-range ($2\le\|i-j\|\le4$ intramolecular)	231
Long-range ($\|i-j\|\ge5$ or intermolecular)	365
Restrained intermolecular hydrogen bonds	11
Total dihedral angle restraints (ϕ/ψ)	22
Structure statistics	Mean ± s.d.
CYANA target function value (Å^2)	2.97 ± 0.28
Violations (mean ± s.d.)	0
Distance restraint violations >0.2 Å	
Dihedral angle restraint violations >5°	0
Deviations from idealized geometry	
Bond lengths (Å)	0
Bond angles (°)	0
Average pairwise r.m.s.d. (Å)[a]	
Backbone N, C^{α}, C′ (Å)	0.39 ± 0.07
Heavy atoms (Å)	0.71 ± 0.08

[a]Pairwise r.m.s.d. was calculated on all of the ten refined structures for residues 3–27.

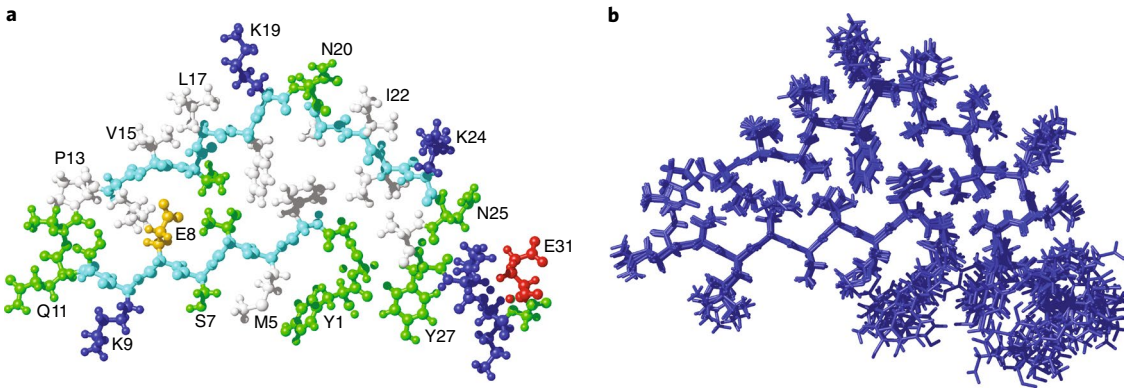

Fig. 2 | 3D structure of a single peptide layer of β-endorphin amyloid protofibrils. a, The lowest energy structure. The amino acid residues are colored white, green, blue and red for hydrophobic, polar, positively charged and negatively charged side chains, respectively. The backbone atoms of the β-strands are colored in cyan. In addition, the side chain of Glu8 is colored in orange to indicate its protonation state (see text). Five positively charged lysine residues protrude from the protofibril surface, which may interact with the negatively charged heparin. **b**, Superposition of the ten conformers representing the NMR structure of β-endorphin.

The N-terminal residues Tyr1 and Gly2 are not assigned and probably not visible in the spectrum, indicating that these residues are flexible. In addition, structural heterogeneity is expected in the vicinity of Gly3, Ile23 and Tyr27 based on the presence of a second set of distinct resonances[23]. Finally, the five positively charged lysine residues and the two terminal residues are part of the solvent-exposed fibril surface (Fig. 3c,d).

The location of Glu8 in the core is unusual, but supported by many NMR restraints to Leu14, Val15 and Thr16 (about 40 manually assigned restraints, including nine spectrally unambiguous ones in Supplementary Table 2). Its low side-chain carbonyl chemical shift of 175.34 ppm suggests that it is protonated, since the corresponding chemical shift of deprotonated glutamate would be expected to be higher than 180 ppm (ref. [41]). With protonation, Glu8 is well embedded in the hydrophilic core and able to form also a hydrogen-bond ladder.

A putative role of Glu8 in the fibril disassembly at neutral pH. The finding that Glu8 is protonated in the hydrophilic core of the β-endorphin fibril grown under secretory granule-relevant acidic conditions (with a pH of 5.5) is interesting in a biological context since the release of the hormone amyloid into the blood is accompanied with a pH change of the milieu from 5.5 to 7.4. This increase in pH may eventually cause the deprotonation of Glu8, along with the destabilization of the fibril core and subsequent fibril disassembly. It could be thus expected that the deprotonation of Glu8 on pH change could provide the mechanism for the decomposition of the fibril and the release of β-endorphin monomers. However, β-endorphin fibrils have shown to be stable at pH values around 7.4 (ref. [34]), which speaks against such a simple mechanism.

To probe in more detail whether Glu8 protonation is indeed relevant for disaggregation of the β-endorphin amyloids, we made two mutations, E8Q and E8L, to replace the negatively charged glutamate side chain with either the polar glutamine or the hydrophobic leucine side chain. Both the E8Q and E8L mutants form amyloid fibrils, as evidenced by electron microscopy (Extended Data Fig. 5). To determine the structural influence of the mutations on the fibril conformation, isotopically labeled E8Q fibrils were prepared and 20 ms dipolar assisted rotational resonance (DARR) spectra were recorded and compared to the 20 ms DARR spectrum of wild-type β-endorphin amyloid. The overlay is shown in Extended Data Fig. 5; the overall appearance of the two spectra is very similar, indicating a quasi-identical 3D fold, although some considerable chemical-shift differences are observed for residues Leu14, Val15, Thr16 and to a lesser extent for Leu17. These chemical-shift differences are expected since these residues are close in space to Glu8 across the fibrillar core.

We then monitored the disassembly of wild-type, E8Q and E8L amyloid fibrils using an in vitro disaggregation assay that mimics the conditions encountered by the β-endorphin fibrils on secretion into the blood by means of the change in pH (ref. [11]). We assembled amyloid fibrils with wild-type and mutant β-endorphins at pH 5.5 (similar to pH inside secretory granules) and in the presence of heparin (see Methods). The amyloid fibrils were shortened by sonication[42] to reach a size of 100–300 nm close to the secretory granule size[11], followed by dialysis with a 10 kDa membrane against 10 mM Tris buffer at pH 6.5, 7.4, 8.5 or 9.5 mimicking the change of pH from the secretory granule (pH 5.5) to the blood environment (pH 7.4) (Fig. 4, Extended Data Fig. 6 and Supplementary Fig. 3). During dialysis, fibrils in all five pH conditions released monomers (Fig. 4, Extended Data Fig. 6 and Supplementary Fig. 3), supporting the observation that hormone fibrils are unstable on dilution by change to a phosphate-free buffer system as documented earlier for heparin-free nonsonicated β-endorphin fibrils[14]. We expect that the release of monomers in the native environment should be a few orders of magnitude higher than what we observe here, under simplified experimental conditions, as discussed in detail below. We note that the tendency of wild-type fibrils to disassemble with increasing pH is more pronounced than for the E8Q and E8L mutants (Fig. 4). The effect is stronger at higher pH (that is, pH 8.5–9.5). indicative of a high pK_a value Glu8 within the fibril. Indeed, we observe a high chemical CO shift at pH 7.4 suggesting that Glu8 is still protonated in the fibril core (Extended Data Fig. 7). At this neutral pH, a particular deprotonation of Glu8 is, however, expected at the end of fibrils as Glu8 gets exposed to the solvent. The number of molecules at the end of the fibrils is very low in comparison to the ones inside the fibril and thus the cross peaks of Glu8 sitting at the fiber endings are not detectable in the solid-state NMR spectra. To assess whether the pH-triggered release of peptides from fibrils involves only the molecules at the end of the fibrils, we compare disassembly of sonicated and nonsonicated long fibrils, and observed more monomer release for the sonicated fibrils, which have more ends per mass than the nonsonicated fibrils, at all pH conditions (Extended Data Fig. 6). Apart from the general dilution effect during dialysis, which causes partial fibril disassembly, our observation at high pH supports the hypothesis that Glu8 functions as a molecular switch that guides the assembly/disassembly of fibrils on pH change.

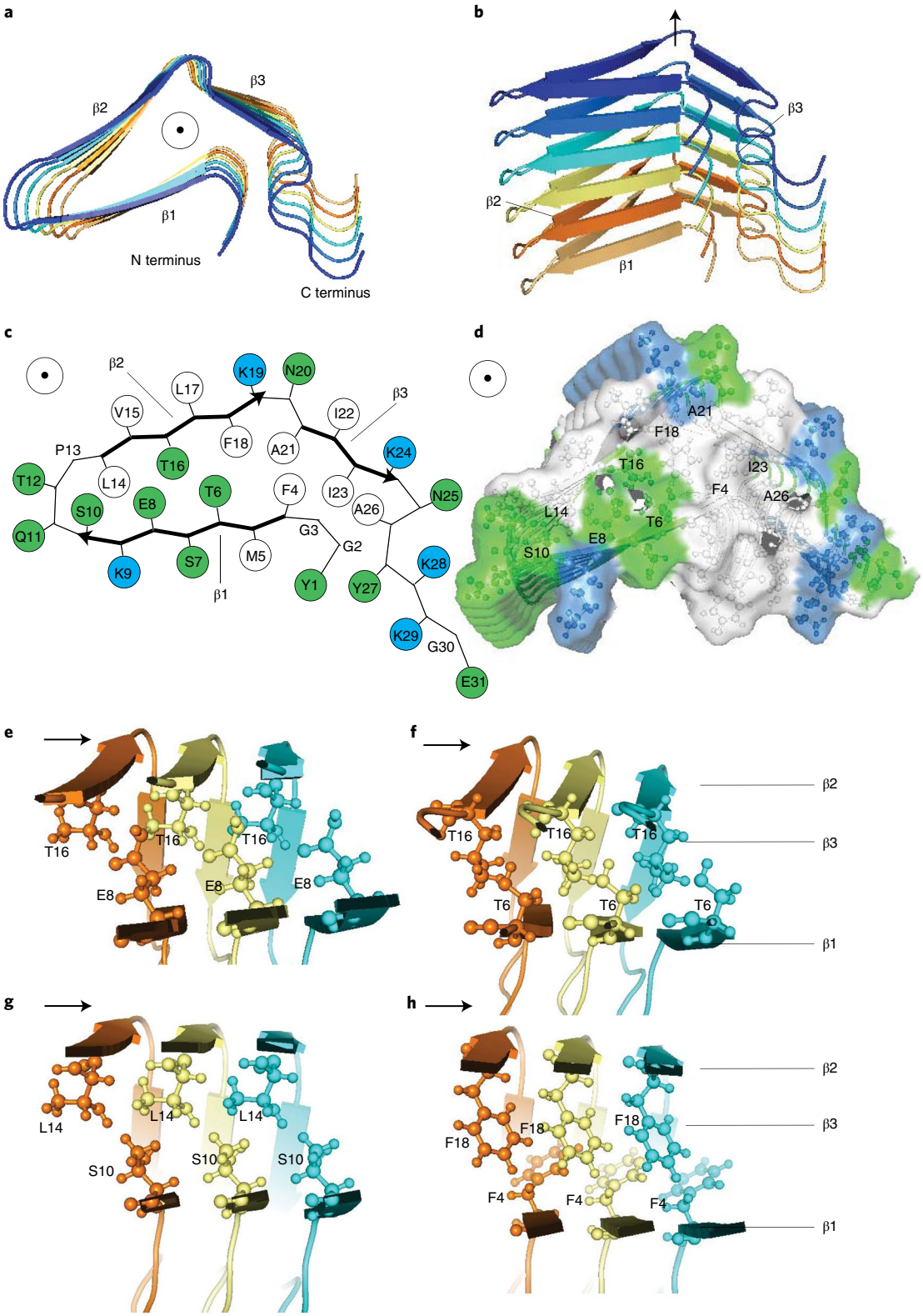

Fig. 3 | 3D structure of β-endorphin amyloid protofibrils. a,**b**, Top (**a**) and side (**b**) views of the β-endorphin protofibril. One layer of the β-solenoid is composed of one peptide. **c**, Schematic structure colored by residue type; white are hydrophobic, green are polar and blue are positively charged residues. The β-strands along the backbone are highlighted with arrows. **d**, Color-coded surface representation of the fibril structure. **e**–**h**, Side views of the intermolecular contacts Glu8–Thr16 (**e**), Thr6–Thr16 (**f**), Ser10–Leu14 (**g**) and Phe4–Phe18 (**h**) contacts.

Discussion

Many proteins including hormones are secreted by the cell through a regulated secretory pathway by which cells are able to store peptide or protein entities for extended periods of time in so-called secretory granules to release very fast and in large amounts the protein or hormone into the blood on triggering[7,8]. The protein or hormone

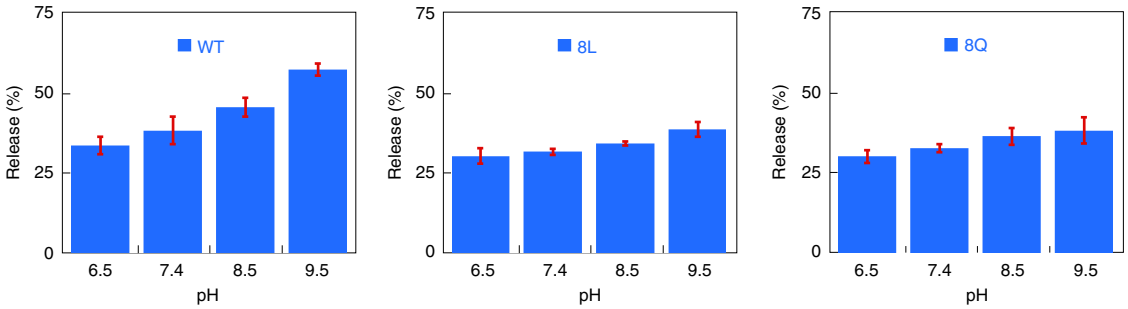

Fig. 4 | Wild-type β-endorphin fibrils disassemble faster with increasing pH than the variants E8L and E8Q. Bar diagram representation of the relative disassembly for sonicated wild-type β-endorphin (WT) fibrils and its variants E8L and E8Q measured at different pH values after 50 h disassembly time in buffer B. The release was measured by UV absorbance at 280 nm outside the dialysis membrane and normalized such that 100% corresponds to the entire peptide material. The data show that with increasing pH, wild-type β-endorphin fibrils disassemble more than those of the mutants E8Q and E8L. For example, at pH 9.5, wild-type β-endorphin fibrils are disassembled to 57 ± 2% release while E8L and E8Q fibrils released only 39 ± 2% and 38 ± 4% through the dialysis membrane, respectively. Data are shown as means and s.d. of $n = 3$ of different samples.

is thereby believed to be stored inside the secretory granule in a functional amyloid state[11,43,44]. Our 3D structure of an amyloid of β-endorphin (Fig. 3) comprises a β-solenoid fold with a hydrophilic surface similar to the other available 3D structures of functional amyloids such as the HET-s(218–289) prion[27,39] and the necrosome RIPK1–RPIK3 amyloid[45]. It is well packed with both a hydrophobic as well as a hydrophilic core, structurally insensitive to small changes in buffer conditions[19], and gives rise to high-resolution-quality solid-state NMR spectra—all properties that are expected for a functional amyloid and that rationalize stable and densely packed hormone storage. The 3D structure shows that the storage container is the peptide itself in a well-defined aggregated state.

An important component of the β-endorphin amyloid fibrils studied here is the presence of heparin as a representative of glycosaminoglycans present in secretory granules[11]. While heparin is absent from the 3D structure due to the lack of experimental restraints, it has an important structural role as demonstrated by Nespovitaya et al.[14,15]. Heparin facilitates β-endorphin fibril formation and stability, and appears to orchestrate the assembly of a single environment-insensitive amyloid polymorph, in contrast to the multiple polymorphs observed for heparin-free β-endorphin amyloids[14]. Moreover, the presence of heparin results in a structure featuring a protonated Glu8 in the fibril core; in absence of heparin, Glu8 is negatively charged and within a different fibril structure, thereby changing the pH sensitivity of fibril disassembly. The super-resolution fluorescence microscopy studies by Nespovitaya et al.[14,15] led to a structural model with heparin as a structural linker between two protofibrils. The presence of natural abundance 1% ^{13}C-labeled heparin signals in the solid-state NMR spectra of the ultra-centrifuged solid-state NMR sample (Extended Data Fig. 8) supports this suggested structural role. The lack of any interprotofibril interactions in the solid-state NMR spectra provides further agreement with the proposed model. Based on the 3D structure (Figs. 2a and 3c) showing the highly conserved, solvent-exposed and positively charged array of lysine residues (Lys19, Lys9, Lys24, Lys28, Lys29); interactions of one or several of them with the negatively charged heparin is plausible. Potential prime candidates are Lys24 and Lys28 since only their Nζ chemical shifts are observed and their chemical-shift values are at rather high-ppm values, both findings are indicative of a close contact with a negatively charged entity. Based on this in vitro observation, one may speculate on a relevant in vivo role of glycosaminoglycans in the formation of β-endorphin fibrils and thus secretory granules.

An essential property of hormone amyloids is their disassembly on release into the blood. As previously demonstrated[11,14], a combination of hormone dilution, changes in pH (from secretory granule pH of 5.5 to the blood pH of 7.4) and in buffer composition (from the intracellular phosphate environment to the carboxylic acid buffer system in the blood) is crucial for amyloid disassembly. The 3D structure of the β-endorphin fibril determined here reveals that the highly conserved Glu8 (Extended Data Fig. 9) is protonated in the amyloid core and acts as a pH sensor. Deprotonation by a pH increase would result in a negatively charged Glu side chain within the core of the amyloid, which would be strongly unfavorable energetically, thus contributing to fibril disassembly. As the pK_a of the carboxyl group of Glu8 is above pH 7.4 (compared to a pK_a of 4.25 of a freely solvent-exposed Glu side chain) as evidenced by the chemical-shift data, at physiological pH, the deprotonation of Glu8 may likely appear only at the water-accessible ends of the fibril releasing a β-endorphin monomer from the fibril end, thereby yielding a controlled release. This view is in line with the rather slow amyloid fibril disassembly observed in vitro (Fig. 4) because the percentage of end molecules per fibril is very low (below 1%) and the dilution factor was rather small.

The 3D structure also points to the amyloid stabilizing role of phosphate[14] or heparin[14,15]. As a poly-anion, phosphate may intercalate between the positively charged Lys side chains arrayed along the fibril surface, thereby reducing their charge repulsion as indicated in the cryo-EM structure of an α-synuclein fibrils polymorph in which a phosphate is likely present between several Lys residues[46], including Lys19, Lys9 and Lys29, with the last one outside the β-solenoid fold. It is thus argued that a change of the buffer, from 60 mM phosphate in the cellular milieu to roughly 1–2 mM phosphate in the blood, would yield an increase of the charge repulsion of the Lys side chains, effectively contributing to β-endorphin fibril destabilization[11,14]. The presence of heparin could have an even stronger effect, since it has a structural role in the β-endorphin fibril, through a proposed interaction with Lys24 and/or Lys28. The concentration of heparin in secretory granules is estimated to be higher (~10 μM–100 mM) compared to the blood (~25 nM–1 μM)[34]. A dilution of the fibril into the blood is therefore expected to destabilize the fibril entity. In summary, the combination of hormone dilution, change in buffer composition and change in pH would promote amyloid disassembly.

Once released, the monomeric β-endorphin is structurally flexible, likely folding into a helix on binding to the receptor and activating it through the highly conserved five N-terminal residues (Extended Data Fig. 9)[47]. In combination with the amyloid structure described here, β-endorphin has chameleon-like structural properties, adopting environment-dependent disordered, helical[44] and β-sheet structures, all of which are believed to be biologically relevant.

In conclusion, the 3D structure of the β-endorphin amyloid fibrils presented here is expected to represent the conformation of the hormone in its storage form inside secretory granules. The complex mechanisms of hormone synthesis, storage, release and activation appear to be guided by the interplay between the structure and the environment. An analogous albeit structurally very different process is spider silk polymerization, which is also triggered by changes in buffer composition and pH conditions, along with shear forces[48]. The reversible nature of the amyloid fibrils formed by β-endorphin and its control by the environmental conditions provides a fascinating illustration of the power and creativity of evolution.

Online content

Any methods, additional references, Nature Research reporting summaries, source data, extended data, supplementary information, acknowledgements, peer review information; details of author contributions and competing interests; and statements of data and code availability are available at https://doi.org/10.1038/s41594-020-00515-z.

Received: 5 March 2020; Accepted: 8 September 2020;
Published online: 12 October 2020

References

1. Chapman, M. R. et al. Role of *Escherichia coli* curli operons in directing amyloid fiber formation. *Science* **295**, 851–855 (2002).
2. Fowler, D. M. et al. Functional amyloid formation within mammalian tissue. *PLoS Biol.* **4**, e6 (2006).
3. Gebbink, M. F. B. G., Claessen, D., Bouma, B., Dijkhuizen, L. & Wösten, H. A. B. Amyloids—a functional coat for microorganisms. *Nat. Rev. Microbiol.* **3**, 333–341 (2005).
4. Maddelein, M. L., Dos Reis, S., Duvezin-Caubet, S., Coulary-Salin, B. & Saupe, S. J. Amyloid aggregates of the HET-s prion protein are infectious. *Proc. Natl Acad. Sci. USA* **99**, 7402–7407 (2002).
5. Maji, S. K., Wang, L., Greenwald, J. & Riek, R. Structure-activity relationship of amyloid fibrils. *FEBS Lett.* **583**, 2610–2617 (2009).
6. Harber, V. J. & Sutton, J. R. Endorphins and exercise. *Sports Med.* **1**, 154–171 (1984).
7. Kelly, R. B. Pathways of protein secretion in eukaryotes. *Science* **230**, 25–32 (1985).
8. Kelly, R. B. From organelle to organelle. *Nature* **326**, 14–15 (1987).
9. Arvan, P. & Castle, D. Sorting and storage during secretory granule biogenesis: looking backward and looking forward. *Biochem. J.* **332**, 593–610 (1998).
10. Dannies, P. S. Concentrating hormones into secretory granules: layers of control. *Mol. Cell. Endocrinol.* **177**, 87–93 (2001).
11. Maji, S. K. et al. Functional amyloids as natural storage of peptide hormones in pituitary secretory granules. *Science* **325**, 328–332 (2009).
12. Gopalswamy, M. et al. Structural characterization of amyloid fibrils from the human parathyroid hormone. *Biochimica et. Biophysica Acta* **1854**, 249–257 (2015).
13. Gelenter, M. D. et al. The peptide hormone glucagon forms amyloid fibrils with two coexisting β-strand conformations. *Nat. Struct. Mol. Biol.* **26**, 592–598 (2019).
14. Nespovitaya, N. et al. Dynamic assembly and disassembly of functional β-endorphin amyloid fibrils. *J. Am. Chem. Soc.* **138**, 846–856 (2016).
15. Nespovitaya, N., Mahou, P., Laine, R. F., Schierle, G. S. K. & Kaminski, C. F. Heparin acts as a structural component of β-endorphin amyloid fibrils rather than a simple aggregation promoter. *Chem. Commun.* **53**, 1273–1276 (2017).
16. Paroutis, P., Touret, N. & Grinstein, S. The pH of the secretory pathway: measurement, determinants, and regulation. *Physiology* **19**, 207–215 (2004).
17. Lagunoff, D. & Rickard, A. Mast cell granule heparin proteoglycan induces lacunae in confluent endothelial cell monolayers. *Am. J. Pathol.* **154**, 1591–1600 (1999).
18. Schuetz, A. et al. Protocols for the sequential solid-state NMR spectroscopic assignment of a uniformly labeled 25 kDa protein: HET-s(1-227). *Chembiochem* **11**, 1543–1551 (2010).
19. Seuring, C. et al. Amyloid fibril polymorphism: almost identical on the atomic level, mesoscopically very different. *J. Phys. Chem. B* **121**, 1783–1792 (2017).
20. Wasmer, C. et al. Infectious and noninfectious amyloids of the HET-s(218-289) prion have different NMR spectra. *Angew. Chem. Int. Ed.* **47**, 5839–5841 (2008).
21. Otzen, D. & Riek, R. Functional amyloids. *Cold Spring Harb. Perspect. Biol.* **11**, a033860 (2019).
22. Seuring, C. et al. Femtosecond X-ray coherent diffraction of aligned amyloid fibrils on low background graphene. *Nat. Comm.* **9**, 1836 (2018).
23. Seuring, C. et al. Solid-state NMR sequential assignment of the β-endorphin peptide in its amyloid form. *Biomol. NMR Assign.* **10**, 259–268 (2016).
24. Wang, Y. J. & Jardetzky, O. Probability-based protein secondary structure identification using combined NMR chemical-shift data. *Protein Sci.* **11**, 852–861 (2002).
25. Wishart, D. S. & Sykes, B. D. The ^{13}C chemical-shift index: a simple method for the identification of protein secondary structure using ^{13}C chemical-shift data. *J. Biomol. NMR* **4**, 171–180 (1994).
26. Riek, R. & Eisenberg, D. S. The activities of amyloids from a structural perspective. *Nature* **539**, 227–235 (2016).
27. Van Melckebeke, H. et al. Atomic-resolution three-dimensional structure of HET-s(218-289) amyloid fibrils by solid-state NMR spectroscopy. *J. Am. Chem. Soc.* **132**, 13765–13775 (2010).
28. Lange, A., Luca, S. & Baldus, M. Structural constraints from proton-mediated rare-spin correlation spectroscopy in rotating solids. *J. Am. Chem. Soc.* **124**, 9704–9705 (2002).
29. De Paëpe, G., Lewandowski, J. R., Loquet, A., Böckmann, A. & Griffin, R. G. Proton assisted recoupling and protein structure determination. *J. Chem. Phys.* **129**, 21 (2008).
30. Bronnimann, C. E., Ridenour, C. F., Kinney, D. R. & Maciel, G. E. 2D ^{1}H-^{13}C heteronuclear correlation spectra of representative organic-solids. *J. Magn. Reson.* **97**, 522–534 (1992).
31. Manolikas, T., Herrmann, T. & Meier, B. H. Protein structure determination from ^{13}C spin-diffusion solid-state NMR spectroscopy. *J. Am. Chem. Soc.* **130**, 3959–3966 (2008).
32. Skinner, S. P. et al. CcpNmr AnalysisAssign: a flexible platform for integrated NMR analysis. *J. Biomol. NMR* **66**, 111–124 (2016).
33. Schütz, A. K. et al. Atomic-resolution three-dimensional structure of amyloid β fibrils bearing the Osaka mutation. *Angew. Chem. Int. Ed.* **54**, 331–335 (2015).
34. Wälti, M. A. et al. Atomic-resolution structure of a disease-relevant Aβ(1–42) amyloid fibril. *Proc. Natl Acad. Sci. USA* **113**, E4976–E4984 (2016).
35. Güntert, P. & Buchner, L. Combined automated NOE assignment and structure calculation with CYANA. *J. Biomol. NMR* **62**, 453–471 (2015).
36. Güntert, P., Mumenthaler, C. & Wüthrich, K. Torsion angle dynamics for NMR structure calculation with the new program DYANA. *J. Mol. Biol.* **273**, 283–298 (1997).
37. Lin, Y.-J., Kirchner, D. K. & Güntert, P. Influence of ^{1}H chemical shift assignments of the interface residues on structure determinations of homodimeric proteins. *J. Magn. Reson.* **222**, 96–104 (2012).
38. Luginbühl, P., Szyperski, T. & Wüthrich, K. Statistical basis for the use of $^{13}C^{\alpha}$ chemical shifts in protein structure determination. *J. Magn. Reson. B* **109**, 229–233 (1995).
39. Wasmer, C. et al. Amyloid fibrils of the HET-s(218-289) prion form a β solenoid with a triangular hydrophobic core. *Science* **319**, 1523–1526 (2008).
40. Nelson, R. et al. Structure of the cross-β spine of amyloid-like fibrils. *Nature* **435**, 773–778 (2005).
41. Platzer, G., Okon, M. & McIntosh, L. P. pH-dependent random coil ^{1}H, ^{13}C, and ^{15}N chemical shifts of the ionizable amino acids: a guide for protein pK_a measurements. *J. Biomol. NMR* **60**, 109–129 (2014).
42. Campioni, S. et al. The presence of an air-water interface affects formation and elongation of α-synuclein fibrils. *J. Am. Chem. Soc.* **136**, 2866–2875 (2014).
43. Soragni, A. et al. Toxicity of eosinophil MBP is repressed by intracellular crystallization and promoted by extracellular aggregation. *Mol. Cell* **57**, 1011–1021 (2015).
44. Seuring, C., Nespovitaya, N., Rutishauser, J., Spiess, M. & Riek, R. in *Amyloid Fibrils and Prefibrillar Aggregates* (ed. Otzen, D. E.) 395–410 (Wiley-VCH, 2013).
45. Mompeán, M. et al. The structure of the necrosome RIPK1-RIPK3 core, a human hetero-amyloid signaling complex. *Cell* **173**, 1244–1253 (2018).
46. Guerrero-Ferreira, R. et al. Cryo-EM structure of alpha-synuclein fibrils. *Elife* **7**, e36402 (2018).
47. Saviano, G., Crescenzi, O., Picone, D., Temussi, P. & Tancredi, T. Solution structure of human β-endorphin in helicogenic solvents: an NMR study. *J. Pept. Sci.* **5**, 410–422 (1999).
48. Hagn, F. et al. A conserved spider silk domain acts as a molecular switch that controls fibre assembly. *Nature* **465**, 239–242 (2010).

Methods

Protein expression and purification. The previously described procedure[19] was used. Briefly, β-endorphin was expressed in *E. coli* BL21* cells (Invitrogen) in a pET32a-vector as a thioredoxin fusion construct with an internal tobacco etch virus- (TEV-)protease cleavage site. With the plasmid inoculated cells were grown at 37 °C in 1 l of ^{13}C,^{15}N-M9, ^{15}N-M9 or ^{13}C-M9 medium if labeled and LB medium if unlabeled. When the cell density reached an optical density (OD_{600}) of 0.8–1.0, protein expression was induced with 1 mM isopropyl-β-D-thiogalactoside and the temperature was decreased to 18 °C. After 16 h of expression, cells were collected by centrifugation and resuspended in lysis buffer A (50 mM Tris pH 8.0, 300 mM NaCl, 20 mM imidazole, 10% v/v glycerol, 1 mM DTT, 0.5 mg lysozyme per ml), then stirred at 4 °C for 10 min and subsequently lysed completely by three passes over a microfluidizer at a processing pressure of 80,000 psi (M-110S, Microfluidics). The supernatant was passed over a 2-cm Ni Sepharose 6 Fast Flow column (GE Healthcare), then washed with 10 column volumes of lysis buffer A and eluted with the same buffer including 200 mM imidazole. For removal of the N-terminal thioredoxin tag, the protein was buffer exchanged into 150 NaCl, 50 mM Tris pH 8, 1 mM DTT on a HiPrep 26/10 desalting column (GE Healthcare) and then treated with inhouse-made TEV protease (1:40 molar ratio) at 20 °C without agitation for at least 7 h. In addition to cleaved, soluble peptide, β-endorphin fusion protein was found in inclusion bodies and purified as described[19].

Fibrillization. Purified β-endorphin was fibrillized as described[19]. In short, β-endorphin was fibrillized at a concentration of 2 mg ml^{-1} in 1.5-ml Eppendorf tubes incubated in an EchoTherm model RT11 rotating mixer (Torrey Pines Scientific) with a speed corresponding to 50 r.p.m. inside a 37 °C incubator. For this purpose, lyophilized β-endorphin was resuspended at a concentration of ~5–10 mg ml−1 in ddH_2O and mixed with 4× fibrillization buffer. Additional ddH_2O was added to yield the final fibrillization concentration of 2 mg ml^{-1} in either Buffer A (10 mM NH_4Ac, 200 mM NaCl, 400 µM LMW heparin (5 kDa heparin from CalBioChem), 0.01% sodium azide, pH 5.5) or Buffer B (5% D-mannitol, 0.01% sodium azide, 400 µM LMW heparin (5 kDa heparin from CalBioChem), pH 5.5). The incubation time for fibril formation was monitored over time measuring the residual soluble material on ultracentrifugation by absorption measurements. The incubation time used was about 2 weeks. This procedure was used for uniformly ^{13}C,^{15}N-labeled samples, mixed ^{13}C,^{15}N (1:1) samples, as well as a 1:4 mixture of ^{13}C,^{15}N and unlabeled samples starting by mixing the individual material at the lyophilized stage.

Solid-state NMR spectroscopy. All solid-state NMR experiments were performed on a Bruker 850 MHz wide-bore magnet using a Bruker 3.2 mm triple-resonance 'E-free' probe. The data was recorded and processed using Topspin 3.2. We recorded three types of 2D ^{13}C-^{13}C correlation experiment with different mixing elements on both the uniformly labeled and the 1:4 diluted sample for the dilution analysis. These mixing elements were a 500-µs CHHC, a 6.5-ms PAR and a 400-ms PDSD. Additionally, a 6 ms 2D ^{13}C-^{15}N PAIN was recorded on the 1:1 ^{13}C:^{15}N-labeled sample. Experiments on both samples were done back-to-back to keep the experimental conditions as similar as possible. Supplementary Table 3 summarizes all experimental conditions. Note that acquisition times were longer on the diluted sample to account for the lower concentration of active isotopes. Peaks were picked using CcpNmr Analysis[32].

Structure calculation. The structure calculations were performed using combined automated distance restraint assignment and structure calculation with CYANA v.3.98.3 using 100,000 torsion angle dynamics steps per conformer[35,36]. In each calculation cycle, 95 structures were calculated and the ten structures with the lowest final target function values were selected for the structural bundle. The restraints and peak lists that were used for the calculation can be found in the Supporting Information (Supplementary Tables 1 and 2).

The structure is well supported by Ramachandran statistics (PROCHECK) with 64.5% of residues in most favored regions and 35.5% in additionally allowed regions.

β-endorphin fibril preparation for the fibril disassembly assay. A 2.5 mg amount of wild-type β-endorphin peptide and its mutants E8L/E8Q (purchased from Bachem, Switzerland) were dissolved in 400 µl in both buffers containing 0.01% sodium azide. heparin (molecular weight of ~5 kDa) was added to the peptide solutions drop-wise, and the final volume of the mixture was adjusted to 500 µl. In the final mixture both peptide and heparin concentration were 1,400 µM. Thereafter, the pH of the solutions was adjusted to 5.5. The resulting solution mixtures were incubated at 37 °C for 7 d for fibrillation with slight agitation.

Fibrillar disassembly assay. Here, 500 µl of every fibril aggregation mixture was either directly used for the fibril disassembly assay or sonicated following procedures as described[42] as follows. The fibrils formed by wild-type β-endorphin and its mutants (E8L/E8Q) were sonicated using probe sonicator and subsequently used for release assay. The fibrils were placed on an ice bath and sonicated for 90 min with constant amplitude of 30% and 30 pulses per min (two pulses on and two pulses off). After 20, 30 and 90 min, 4 µl of the sonicated samples were taken and subjected to electron microscopy analysis. Finally, sonicated samples obtained after 90 min were selected for the release assay, centrifuged at 20,000*g* for 90 min at 4 °C to obtain 'pure' short fibrils. The fibril pellets were resuspended in the corresponding buffer A or B and the final peptide concentrations were adjusted to 800 µM monomer concentration. The solution was then subjected to dialysis through a 10 kDa cut-off membrane against 500 µl of 10 mM Tris HCl buffer (pH 6.5, 7.4, 8.5 and 9.5). Then, 250-µl fibril samples were placed into a Slide-A-Lyzer mini dialysis unit system (Thermo Fisher Scientific), capped and positioned into a home-made dialysis tube containing 500 µl of Tris HCl buffer (pH 6.5, 7.4, 8.5 and 9.5). The Slide-A-Lyzer dialysis unit was placed such that its membrane was in contact with the buffer. Magnetic bars were put into individual tubes and the assembled units were placed on a magnetic stirrer. The rotation of the magnetic bars provided a constant movement in the outer solution allowing release of monomer. After suitable time intervals (0, 15, 24, 36 and 50 h), the solutions outside the dialysis membrane were taken for analysis. To monitor the monomer release/fibrillar disassembly, an aliquot of 150 µl solution from the dialysis tube (outside the membrane) was taken and absorbance in the ultraviolet (UV) range (240–340 nm) was measured. After each reading, the outside solution was returned to the dialysis tube and the dialysis systems were reassembled. Absorbance at 280 nm for different time points were taken; normalized with respect to its absorbance at 0 h and plotted against time for wild-type β-endorphin and its mutants (E8L/E8Q) across different pH values.

Reporting Summary. Further information on research design is available in the Nature Research Reporting Summary linked to this article.

Data availability

Structural coordinates and experimental restraints have been deposited in the wwPBD under accession code PDB 6TUB. NMR chemical shifts have been deposited in the BMRB under entry 26715.

Acknowledgements

We thank ETH and the Swiss National Science Foundation for financial support.

Author contributions

C.S., N.N., M.A.W., D.G. and R.C. prepared samples. C.S., J.V., D.G., S.K.M., B.H.M. and R.R. planned the research. C.S., J.V., J.G. and D.G. collected and analyzed data. C.S., J.V., J.G., B.H.M., R.R. and P.G. analyzed NMR data and performed structure calculations. C.S., J.V., P.G., S.K.M., B.H.M. and R.R. wrote the paper.

Competing interests

The authors declare no competing interests.

Additional information

Extended data is available for this paper at https://doi.org/10.1038/s41594-020-00515-z.

Supplementary information is available for this paper at https://doi.org/10.1038/s41594-020-00515-z.

Correspondence and requests for materials should be addressed to B.H.M. or R.R.

Peer review information Inês Chen was the primary editor on this article and managed its editorial process and peer review in collaboration with the rest of the editorial team.

Reprints and permissions information is available at www.nature.com/reprints.

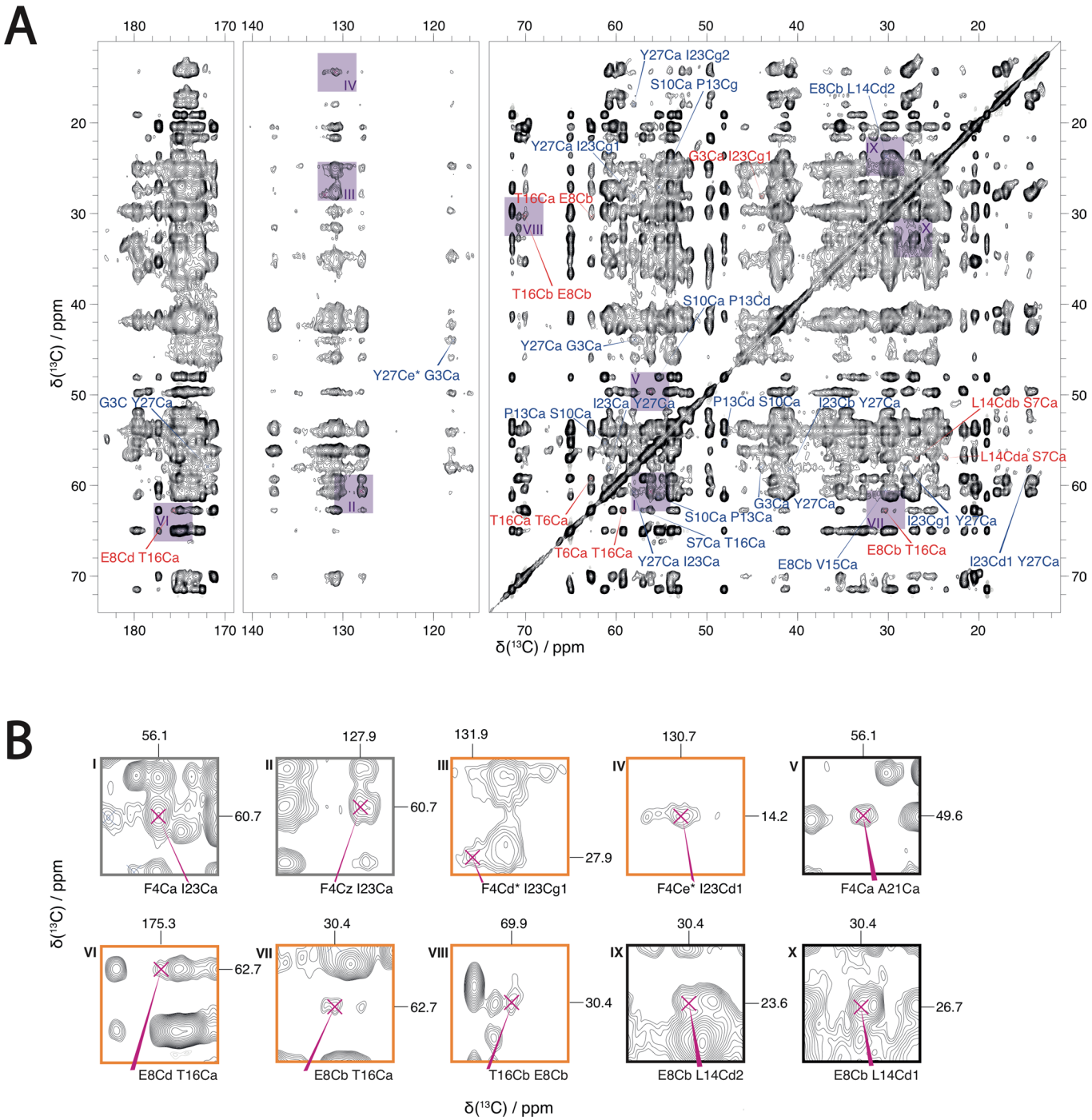

Extended Data Fig. 1 | NMR spectrum for distance restraint collection: 400 ms PDSD spectrum recorded on uniformly $^{15}N,^{13}C$-labelled fibrils . **a**, Spectrally unambiguous contacts are labeled in red for intermolecular contacts and in blue for contacts that are ambiguous with respect to being intra- or intermolecular. Some structurally relevant restraints defining crucial contacts in the 3D fold of the protein (Supplementary Table 2, PDSD) were assigned manually and are shown in **b** as zoomed-in regions: E8 sidechain to L14, E8 to T16; F4 sidechain to A21 and I23. Intramolecular contacts are framed in grey, intermolecular contacts in orange. Contacts that are ambiguous with respect to being intra- or intermolecular are framed in black.

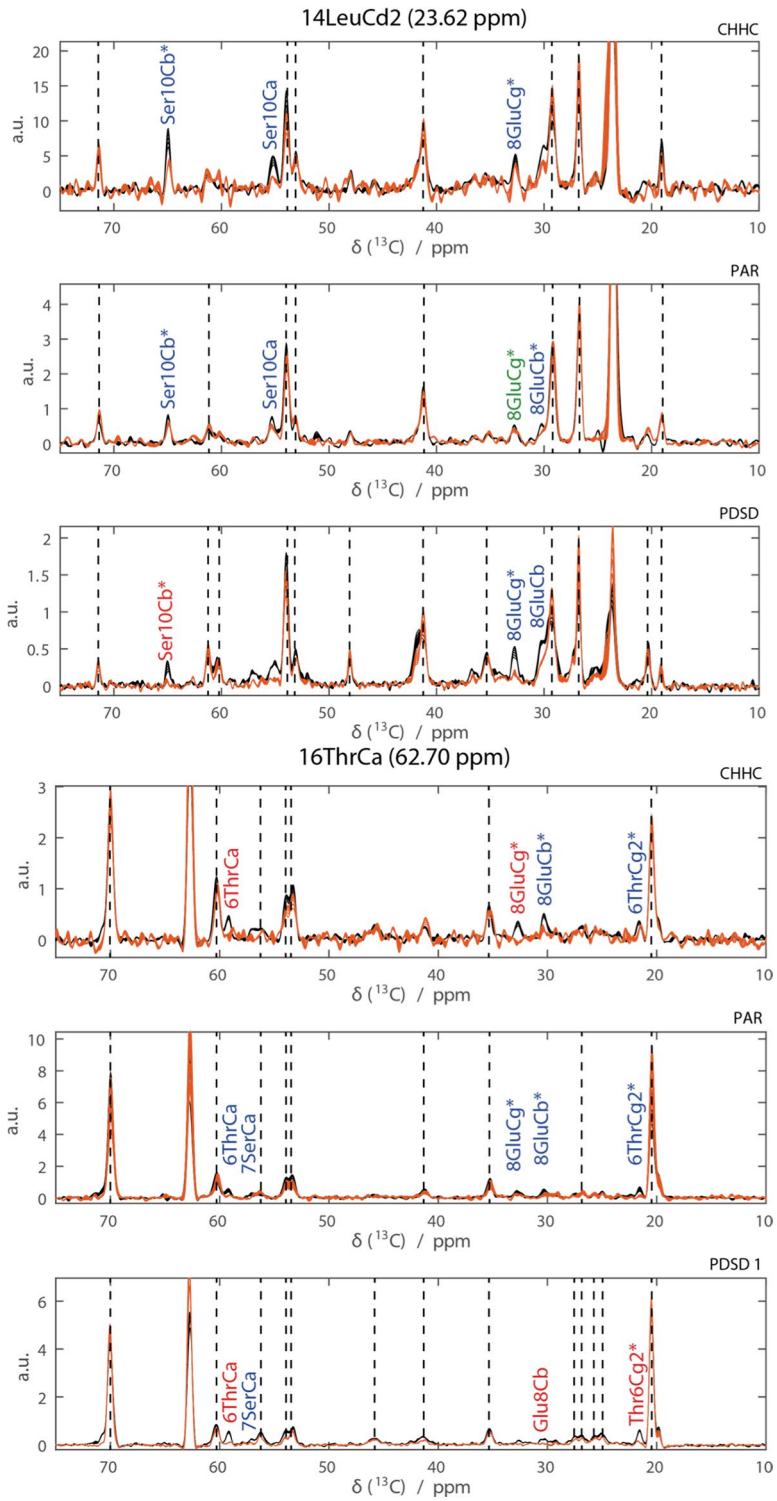

Extended Data Fig. 2 | See next page for caption.

Extended Data Fig. 2 | Spectral distinction between inter and intra-molecular contacts. Selected traces through the indirect dimension of the individual spectra (as indicated on the right) of a fully uniformly $^{13}C,^{15}N$-labeled sample in black and a sample diluted four-fold with unlabeled peptide in red at the resonance frequencies of 14LeuCD2 (23.62 ppm, three top panels) or 16ThrCA (62.70 ppm, three bottom panels) as indicated. The dashed lines indicate the peaks that were used for scaling. Red labels are used for intermolecular contacts, green labels for intramolecular contacts, and blue labels for contacts that fall in between. In short, if the relative cross peak intensity in the spectra of the diluted sample is similar in intensity as the one in the spectrum of the fully-labeled sample (see green-labeled cross peak 8GluCG) the cross peak originates from an intra-molecular contact, while an inter-molecular contact would give rise to a 5-fold less intense cross peak attributed to the dilution (see, for instance, the red-labeled cross peak 6ThrCA). Signal intensities in the two spectra to be compared (uniformly labelled versus diluted) were determined by summing over the peak regions in a 0.5 by 0.5 ppm square centered at the peak positions. The noise on these signal intensities was estimated by the standard deviation of a set of 1000 signal intensities in an empty region of the spectrum. For each slice j, a scaling factor $S_j = \left(\sum_i w_i U_i/D_i\right) / \left(\sum_i w_i\right)$ was determined, where the sums run over all peaks in slice j, U_i and D_i are the intensities of a given peak i in the uniformly labelled and diluted spectrum, respectively, and $w_i = 1/\sigma_i^2$ with σ_i equal to the error of the intensity ratio obtained by error propagation from the estimated noise of the intensities. For each peak i in slice j that spans more than 2 residues, the scaled intensity ratio $R_i = S_j D_i/U_i$ and its error σ_{R_i}, obtained by error propagation, were computed. Restraints were classified as intramolecular if $R_i + \sigma_{R_i} > 0.8$ and $R_i - \sigma_{R_i} > 0.7$, or as intermolecular if $R_i + \sigma_{R_i} < 0.4$ and $R_i - \sigma_{R_i} < 0.3$. Ratios that do not meet either of these criteria are classified as ambiguous with respect to being an intra- or intermolecular restraint.

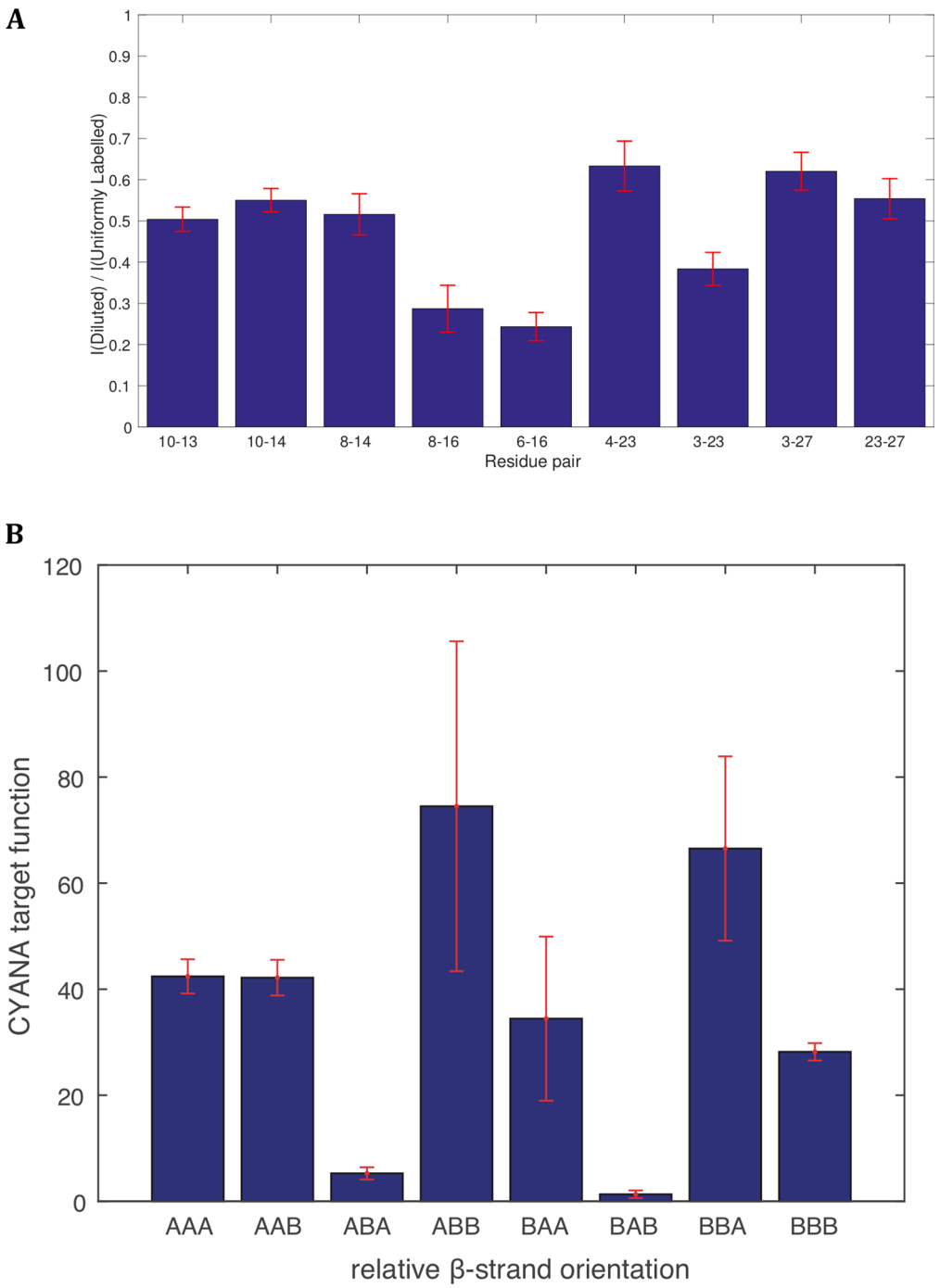

Extended Data Fig. 3 | See next page for caption.

Extended Data Fig. 3 | The identification of the staggering extent (A) and of the relative orientation of the β-sheets (B). The weighted mean ratio between relative cross peak intensities from spectra obtained of a fully uniformly ^{15}N,^{13}C-labeled sample and a 80% (1:4) diluted sample (shown in part in Extended Data Fig. 2 and Supplementary Fig. 4) are shown per residue pair (as indicated on the x-axis). The weighted mean ratios were obtained by averaging over all cross peaks observed between the two residues in the various spectra, weighing the contribution of the *i*-th cross peak by $1/\sigma_i^2$, where σ_i is the error of the peak intensity ratio for cross peak *i*. Error bars show the estimated standard error of the weighted mean, determined by performing a bootstrap with a sample size of 10,000. If the cross peaks between a residue pair is due to an intra-molecular interaction, the value should be 1, if it is of entire inter-molecular origin, the value should be 0.2. In a staggered structure, individual contacts across the fibrillar core can have an intra- or intermolecular nature. However, the weighted average of all contacts for a cross fibrillar-core contacts should tend towards a value in between the intra- and intermolecular regime. Here, these ratios are all substantially lower than 1 and mostly higher than 0.2, indicating that the structure is indeed staggered. Once the in-register parallel β-sheet conformation has been established, the relative orientation of the β-sheets, that is the direction of the hydrogen bonds along the fibril axis (N-H···O=C, denoted here as A, or C=O…H-N, denoted here as B), was determined. Four unique possibilities for the relative orientation of the three β-strands β1, β2, β3 exist (Supplementary Fig. 4). These are labeled with AAA, AAB, ABA, and ABB. (The BBB orientation is equivalent to AAA, BAB to ABA, BBA to AAB, and BAA to ABB.) CYANA structure calculations of β-endorphin fibrils were performed with all four orientations of the β-sheets using in addition to the experimental restraints for each of the possible orientations their corresponding intermolecular hydrogen-bond restraints. The plot shows the CYANA target function value, which is a weighted sum of all squared restraint violations. Only the ABA (and equivalent BAB) orientation yielded a low target function value and thus a well fulfillment of the experimental restraints and therefore the ABA orientation was used in the subsequent final structure calculations. ABA is the one arrangement for which the hydrogen bonds of β-sheet β2 have the opposite orientations along the fibril axis to the β -sheets β1 and β3 strands.

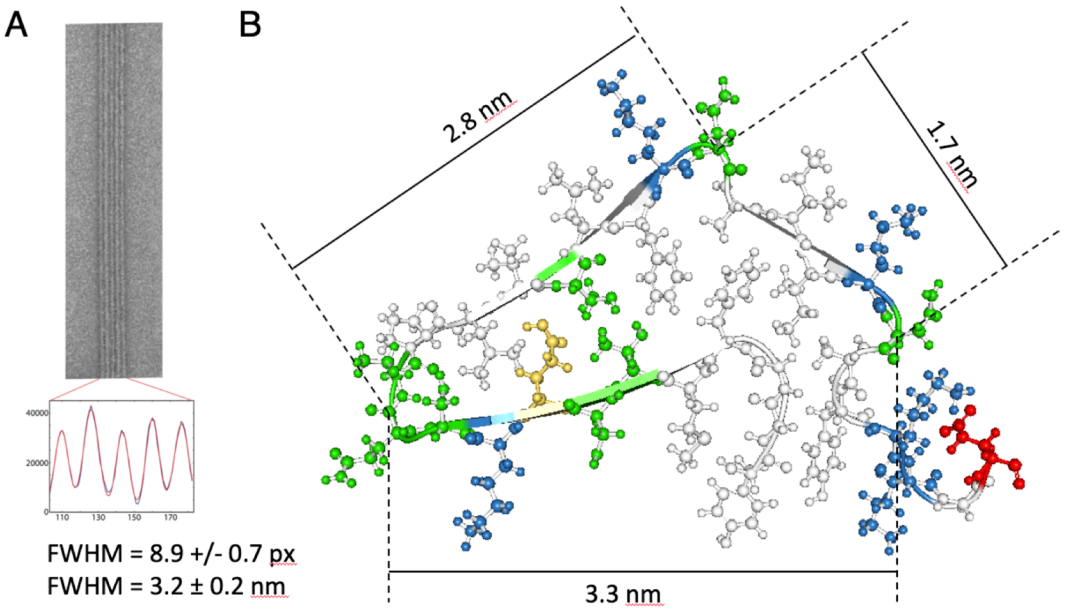

Extended Data Fig. 4 | Embedment of the 3D structure of the proto-fibril into the fibril. The width of 3.2 +/− 0.2 nm of proto-fibrils within fibrils extracted from (**a**) negative-stain transmission electron microscopy data from Seuring et al. 2017 (ref. [19]) fit well (**b**) the dimension of the determined 3D solid state NMR structure. In the depicted micrographs, β-endorphin forms straight, striated fibril ribbons of variable widths in buffer A. The full width at half-maximum (FWHM) of approximately 3 nm (9 pixels) can be retrieved from the corresponding intensity profiles.

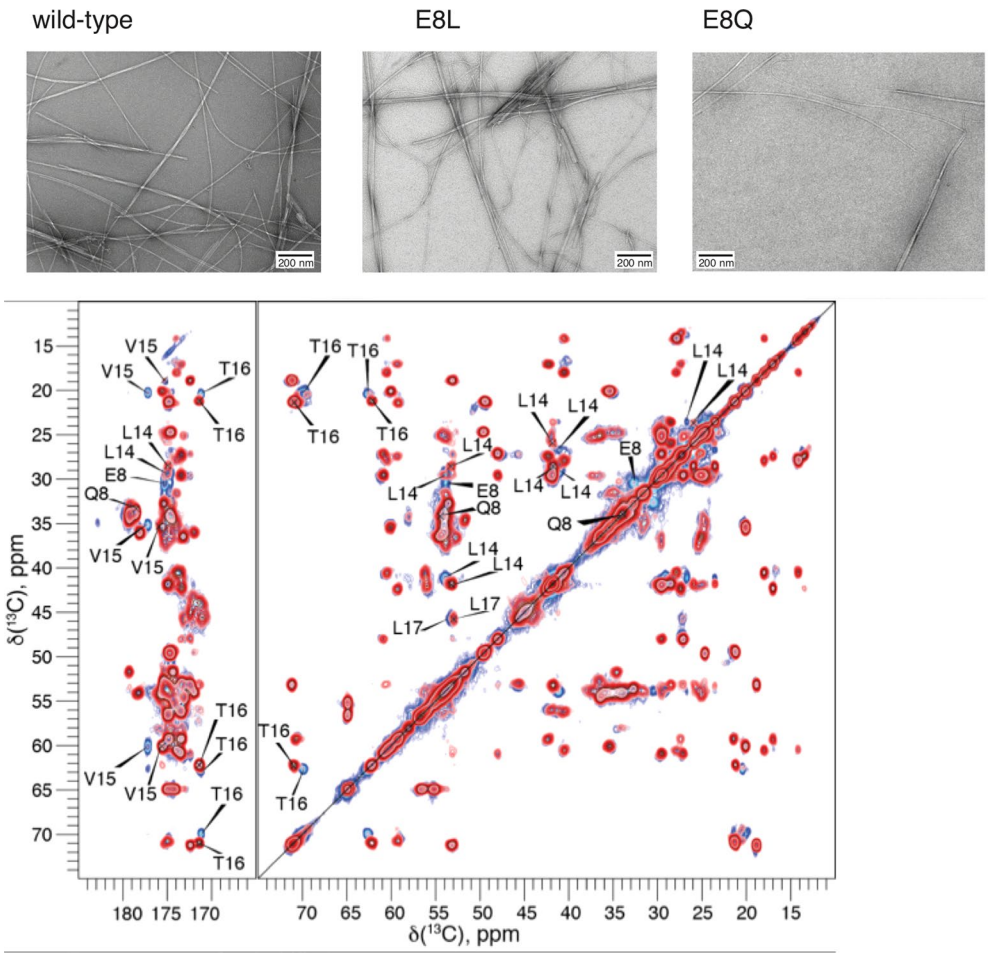

Extended Data Fig. 5 | Negative-stain transmission electron micrographs and NMR spectra show that the two variants E8L and E8Q form also amyloid fibrils with similar morphologies and 3D structure as wild type β-endorphin. Negatively stained transmission electron micrographs of wild-type β-endorphin and the two variants E8L and E8Q are shown (all prepared in buffer B). Scale bars correspond to 200 nm. Below, a superposition of the 20 ms [^{13}C,^{13}C]-DARR spectra of wild type β-endorphin (blue) and the variant E8Q (red) is shown. The close resemblance between the two spectra indicates the formation of the same fold. Only residues in spatial proximity to residue 8, that is Leu14, Val15, Thr16, and, to a lesser extent, Leu17 show significant chemical shift changes. The cross peaks for which the chemical shift perturbation due to the mutation exceeds the line width, are labeled for both the wild-type and the variant E8Q amyloid fibrils with one letter amino acid residue codes. The line widths are overall comparable between the two spectra, indicating homogeneous samples for both endorphin forms. The spectrum of wild type β-endorphin fibrils was recorded at 20.0 T static magnetic field and 17 kHz MAS. The spectrum of the mutant E8Q was recorded at 14.1 T static magnetic field and 13 kHz MAS.

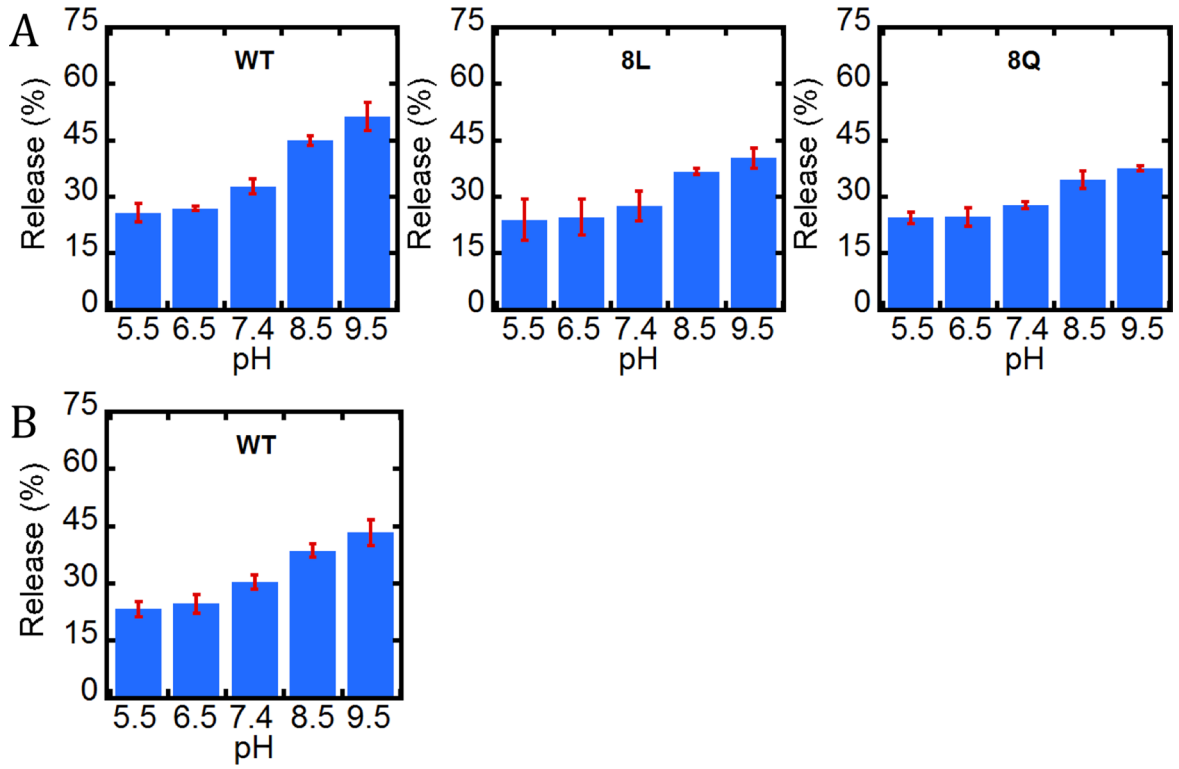

Extended Data Fig. 6 | Fibril disassembly of wild type and mutant β-endorphin fibrils in absence (A) and presence (B) of sonication in the acetate buffer A. a, **b**, Bar diagram representation of the relative disassembly for (**a**) sonicated and (**b**) not-sonicated wild type β-endorphin (WT) fibrils and in (**a**) also its variants E8L (8L) and E8Q (8Q) measured at different pH values after 50 h disassembly time. The release was measured by UV absorbance at 280 nm outside the dialysis membrane and normalized such that 100% corresponds to the entire peptide material. The data show that with increasing pH, wild type β-endorphin fibrils disassemble more than those of the mutants E8Q and E8L. In addition, the disassembly is more pronounced in the sonicated wild type fibrils than the non sonicated ones indicating disassembly also from the end of the fibrils.

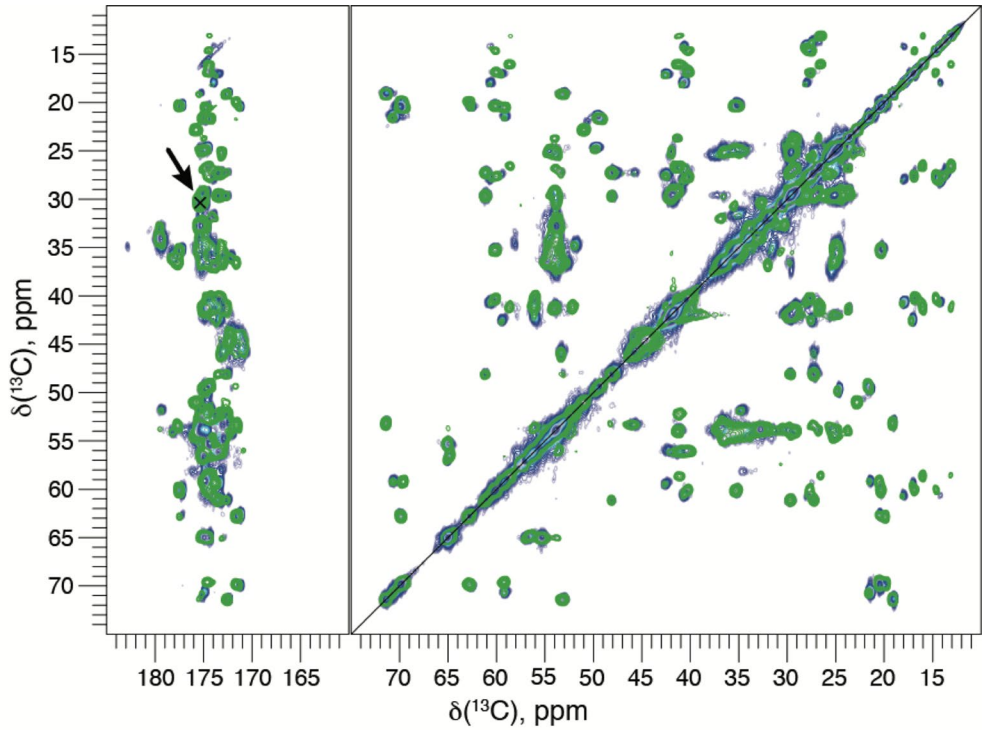

Extended Data Fig. 7 | Glu8 is protonated at pH 5.5–7.4 as evidenced by solid state NMR. 20 ms DARR spectra of wild type β-endorphin amyloids at pH 5.5 (blue) and 7.4 (green) are shown. The arrow highlights the Glu8 C^{δ}/C^{β} cross-peak, which is present in both spectra. The C^{δ} chemical shift indicates the protonated state of the Glu8 carboxyl group.

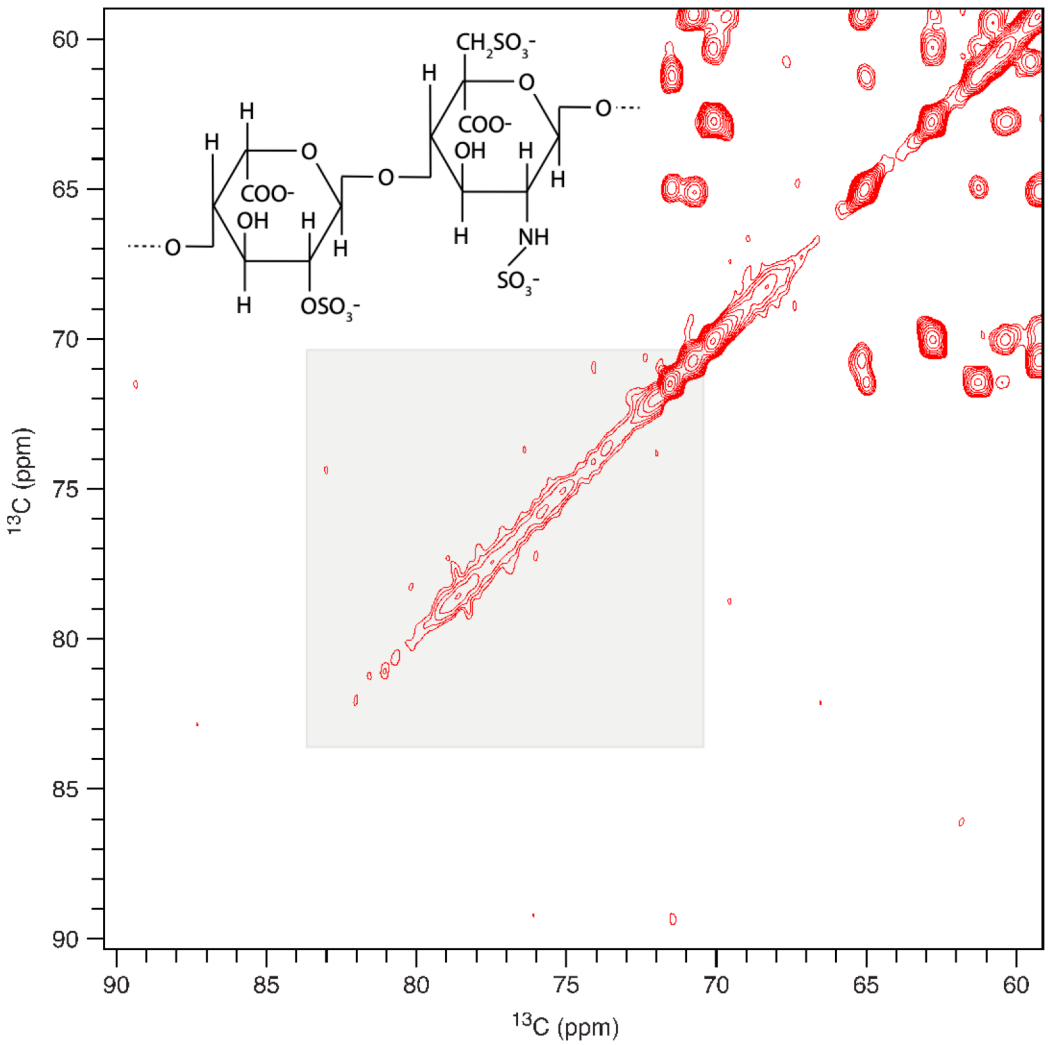

Extended Data Fig. 8 | Presence of natural abundance heparin in the β-endorphin NMR sample as measured by solid state NMR. A weak diagonal signal from natural abundance (1%) ^{13}C heparin indicated by the grey rectangle is observed in the 400 ms [^{13}C,^{13}C]-PDSD spectrum in addition to the strong signals from ^{15}N,^{13}C-labeled β-endorphin amyloids.

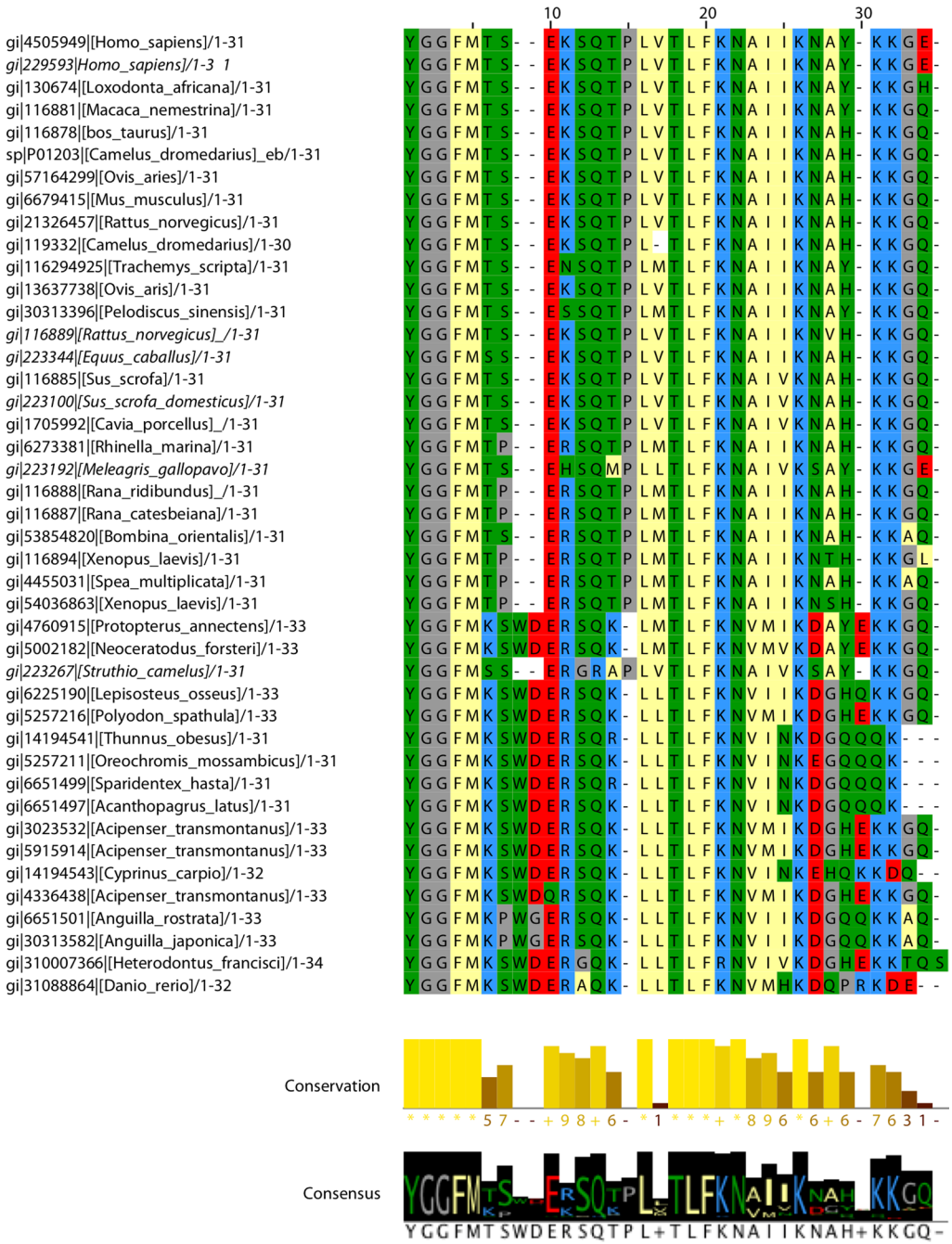

Extended Data Fig. 9 | Sequence alignment of β-endorphins. The 37 sequences shown in this alignment are the non-redundant output of a PSI-BLAST search with the β-endorphin sequence comprising residues 1–31 (carried to convergence at an *E*-value threshold of 0.005). The query sequence is shown as the first sequence of the alignment. Of the other sequences displayed, 31 correspond to β-endorphin sequences of the precursor POMC. The six "only"-β-endorphin sequences are marked by black dots on the left. The color code represents hydrophilic, hydrophobic, negative and positive charged residues in green, white, blue and red, respectively. The consensus and sequence conservations are displayed below. The high conservation of the five N-terminal residues is attributed to their role in receptor activation.

nature research

Corresponding author(s): Prof. Roland Riek (ETH Zurich)

Last updated by author(s): Aug 21, 2020

Reporting Summary

Nature Research wishes to improve the reproducibility of the work that we publish. This form provides structure for consistency and transparency in reporting. For further information on Nature Research policies, see Authors & Referees and the Editorial Policy Checklist.

Statistics

For all statistical analyses, confirm that the following items are present in the figure legend, table legend, main text, or Methods section.

n/a	Confirmed	
☒	☐	The exact sample size (*n*) for each experimental group/condition, given as a discrete number and unit of measurement
☐	☒	A statement on whether measurements were taken from distinct samples or whether the same sample was measured repeatedly
☒	☐	The statistical test(s) used AND whether they are one- or two-sided *Only common tests should be described solely by name; describe more complex techniques in the Methods section.*
☒	☐	A description of all covariates tested
☒	☐	A description of any assumptions or corrections, such as tests of normality and adjustment for multiple comparisons
☒	☐	A full description of the statistical parameters including central tendency (e.g. means) or other basic estimates (e.g. regression coefficient) AND variation (e.g. standard deviation) or associated estimates of uncertainty (e.g. confidence intervals)
☒	☐	For null hypothesis testing, the test statistic (e.g. *F*, *t*, *r*) with confidence intervals, effect sizes, degrees of freedom and *P* value noted *Give P values as exact values whenever suitable.*
☒	☐	For Bayesian analysis, information on the choice of priors and Markov chain Monte Carlo settings
☒	☐	For hierarchical and complex designs, identification of the appropriate level for tests and full reporting of outcomes
☒	☐	Estimates of effect sizes (e.g. Cohen's *d*, Pearson's *r*), indicating how they were calculated

Our web collection on statistics for biologists contains articles on many of the points above.

Software and code

Policy information about availability of computer code

Data collection	Topspin 3.2
Data analysis	CcpNmr Analysis 2.4, CYANA 3.98.3

For manuscripts utilizing custom algorithms or software that are central to the research but not yet described in published literature, software must be made available to editors/reviewers. We strongly encourage code deposition in a community repository (e.g. GitHub). See the Nature Research guidelines for submitting code & software for further information.

Data

Policy information about availability of data

All manuscripts must include a data availability statement. This statement should provide the following information, where applicable:

- Accession codes, unique identifiers, or web links for publicly available datasets
- A list of figures that have associated raw data
- A description of any restrictions on data availability

Structural coordinates and experimental restraints have been deposited in the Protein Data Bank under accession code PDB 6TUB. NMR chemical shifts have been deposited in the Biological Magnetic Resonance Bank (BMRB) under entry 26715. Other data generated or analyzed during this study are available upon reasonable request.

Field-specific reporting

Please select the one below that is the best fit for your research. If you are not sure, read the appropriate sections before making your selection.

☒ Life sciences ☐ Behavioural & social sciences ☐ Ecological, evolutionary & environmental sciences

For a reference copy of the document with all sections, see nature.com/documents/nr-reporting-summary-flat.pdf

Life sciences study design

All studies must disclose on these points even when the disclosure is negative.

Sample size	Structural studies were carried out with more than 10 mg of b-endorphin prepared from unlabeled and uniformly 13C,15N-labeled samples, mixed 13C,15N (1:1) samples, as well as a 1:4 mixture of 13C,15N and unlabeled samples.
Data exclusions	No data was excluded.
Replication	Fibrillar disassembly experiment. It was crucial to make the fibrils very short hence the sonication. Two independent experiments were performed and averaged for each set.
Randomization	Randomization was not relevant in this study.
Blinding	Blinding was not relevant in this structural study.

Reporting for specific materials, systems and methods

We require information from authors about some types of materials, experimental systems and methods used in many studies. Here, indicate whether each material, system or method listed is relevant to your study. If you are not sure if a list item applies to your research, read the appropriate section before selecting a response.

Materials & experimental systems

n/a	Involved in the study
☒	☐ Antibodies
☒	☐ Eukaryotic cell lines
☒	☐ Palaeontology
☒	☐ Animals and other organisms
☒	☐ Human research participants
☒	☐ Clinical data

Methods

n/a	Involved in the study
☒	☐ ChIP-seq
☒	☐ Flow cytometry
☒	☐ MRI-based neuroimaging